Analytica Chimica Acta 1193 (2022) 339318

Contents lists available at ScienceDirect

Analytica Chimica Acta

journal homepage: www.elsevier.com/locate/aca

Optimisation of saliva volumes for lipidomic analysis by nanoflow ultrahigh performance liquid chromatography-tandem mass spectrometry

Gwang Bin Lee [a], Ayse Caner [b, c], Myeong Hee Moon [a, *]

[a] Department of Chemistry, Yonsei University, 50 Yonsei-ro, Seoul, 03722, South Korea
[b] Cancer Research Center, Ege University, 35100, Bornova, Izmir, Turkey
[c] Department of Parasitology, Ege University Medical Faculty, 35100, Bornova, Izmir, Turkey

HIGHLIGHTS

- The effect of initial sample volume on salivary lipid extraction was investigated.
- Optimisation was based on extraction recovery, matrix effect, and quantifiable lipids.
- Of 780 identified lipids, 372 were quantified using nUHPLC-ESI-MS/MS.
- Comprehensive qualitative and quantitative analyses of saliva lipids are reported.
- The minimum sample volume suggested for salivary lipid analysis is 0.5 mL.

GRAPHICAL ABSTRACT

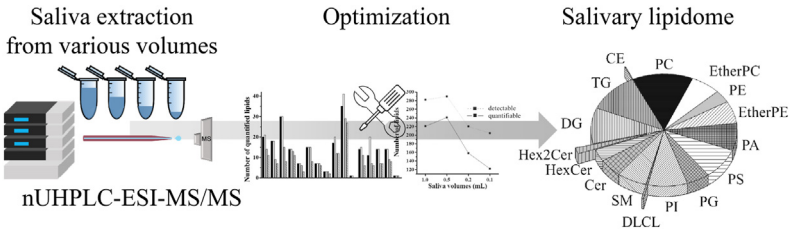

ARTICLE INFO

Article history:
Received 23 August 2021
Received in revised form
10 November 2021
Accepted 21 November 2021
Available online 23 November 2021

Keywords:
Saliva
Lipidomic analysis
Saliva volume
nUHPLC-ESI-MS/MS
Mass spectrometry

ABSTRACT

Saliva is a readily accessible and clinically useful biofluid that can be used to develop disease biomarkers because of a variety of biologically active molecules in it that are also found in blood. However, even though saliva sampling is simple and non-invasive, few studies have investigated the use of salivary lipids as biomarkers, and the extraction of lipids from saliva needs to be examined thoroughly. In the present study, methods (i.e., saliva sample volume, 0.1−1.0 mL) for the extraction and analysis of salivary lipids by nanoflow ultrahigh performance liquid chromatography-tandem mass spectrometry (nUHPLC-ESI-MS/MS) were evaluated according to the matrix effect, extraction recovery, and number of quantifiable lipids. A total of 780 lipids were identified in a pooled saliva sample from 20 healthy volunteers, and 372 lipids without differentiating acyl chain structures were quantified, along with comprehensive information on salivary lipid composition and individual lipid levels. Even though extraction recovery was maintained at saliva sample volumes as low as 0.2 mL, the matrix effect and limit of detection (LOD) were relatively large with 1.0 mL. Considering the matrix effect, LOD, and number of quantifiable lipids

Abbreviations: BEH, ethylene bridged hybrid; Cer, ceramide; CE, cholesteryl ester; CL, cardiolipin; DG, diacylglycerol; HexCer, hexosylceramide; Hex2Cer, dihexosylceramide; IPA, isopropanol; LPA, lysophosphatidic acid; LPC, lysophosphatidylcholine; LPE, lysophosphatidylethanolamine; LPG, lysophosphatidylglycerol; LPI, lysophosphatidylinositol; LPS, lysophosphatidylserine; MTBE, methyl-*tert*-butyl ether; nUHPLC-ESI-MS/MS, nanoflow ultrahigh performance liquid chromatography-tandem mass spectrometry; PA, phosphatidic acid; PC, phosphatidylcholine; PE, phosphatidylethanolamine; PG, phosphatidylglycerol; PS, phosphatidylserine; PI, phosphatidylinositol; TG, triacylglycerol.

* Corresponding author.
E-mail address: mhmoon@yonsei.ac.kr (M.H. Moon).

https://doi.org/10.1016/j.aca.2021.339318

(>limit of quantitation), the minimum volume of saliva sufficient for lipidomic analysis using nUHPLC-ESI-MS/MS was determined to be 0.5 mL.

1. Introduction

Saliva is a clinically informative biofluid that contains a variety of biologically important molecules, including enzymes, proteins, metabolites, nucleic acids, peptides, immunoglobulins, mucins, and lipids [1–5]. Indeed, since such molecules are transferred from the blood to saliva by penetrating spaces between cells *via* transcellular or paracellular routes, most metabolites found in blood serum and urine are also found in saliva [6]. Therefore, like blood and urine, saliva provides a reflection of the physiological status of the body and can be utilised for diagnosing, monitoring, and predicting disease status [6–8]. Furthermore, due to a simple and non-invasive collection of saliva samples, saliva might also be useful for the development of biomarkers. To date, studies have used saliva analysis to monitor the progression of oral diseases [9,10] and to measure levels of a variety of molecules, including drugs [11], nicotine [12], and hormones (e.g., cortisol) [13,14]. Salivary proteins have also been characterised in detail [15]. However, apart from cholesterol, triglycerides, high-density lipoprotein cholesterol, and low-density lipoprotein cholesterol [16,17], salivary lipids, which are essential components of salivary metabolites, have yet to be fully investigated at the molecular level. Therefore, it is important to investigate disease-related perturbations in salivary lipid profiles.

Lipids are involved in a wide variety of cellular functions, including energy storage, intercellular signal transduction, and the regulation of various metabolism [18,19] and are highly complex and diverse, in regards to chain length, degree of unsaturation, and polar head groups, with tens of thousands of lipid molecules that have been reported. In addition, aberrant lipid metabolism has been associated with a number of human lifestyle-related diseases, including atherosclerosis, diabetes, cancer, and neurodegenerative diseases [20–23]. Therefore**, c**hanges in lipid levels and composition have been recognised as potential biomarkers for disease diagnosis and early detection. Recent advancements in liquid chromatography-mass spectrometry (LC-MS) have also facilitated the comprehensive analysis of lipid profiles and the detection of alterations in lipid profiles at the molecular level. Thus, lipidomics has gained interests for developing biomarkers for the diagnosis and prognosis of diseases.

However, even though salivary lipidomics has great potential, the roles and composition of salivary lipids are not well understood. Since saliva is very dilute and is mostly (>99%) water [2], the minimum volume of saliva required for lipid extraction and analysis based on LC-MS has not yet been established. As the initial volume of saliva is reduced, the number of identified lipids is expected to decrease, along with the quantifiable number of lipids. Thus, the aim of the present study was to optimise saliva volumes for lipid extraction and analysis using nanoflow ultrahigh performance liquid chromatography-tandem mass spectrometry (nUHPLC-ESI-MS/MS). More specifically, the effectiveness of lipid extraction from various saliva volumes (1.0–0.1 mL) was evaluated by assessing extraction recovery, matrix effect, limit of detection (LOD), and number of quantifiable lipids based on the limit of quantitation (LOQ) for 24 different lipid classes. Based on saliva volume optimisation, comprehensive information on salivary lipid composition and individual lipid levels is reported.

2. Materials and methods

2.1. Materials and reagents

Lipid standards (n = 64) were purchased from Avanti Polar Lipids, Inc. (Alabaster, AL, USA): lysophosphatidylcholine (LPC) 12:0, LPC 16:0, LPC 17:1, LPC 18:1-D_7, phosphatidylcholine (PC) 12:0/12:0, PC 14:0/16:0, PC 15:0/18:1-D_7, PC 16:0/16:0, PC 17:0/17:0, PC 18:0/18:1, plasmenyl PC P-18:0/18:1-D_9, plasmenyl PC P-18:1/18:1, lysophosphatidylethanolamine (LPE) 14:0, LPE 17:1, LPE 18:0, LPE 18:1-D_7, phosphatidylethanolamine (PE) 12:0/12:0, PE 15:0/18:1-D_7, PE 16:0/16:0, PE 17:0/17:0, plasmenyl PE P-18:0/18:1-D_9, plasmenyl PE P-18:1/18:1, lysophosphatidic acid (LPA) 17:0, LPA 17:1, LPA 18:0, phosphatidic acid (PA) 14:0/14:0, PA 15:0/18:1-D_7, PA 17:0/17:0, lysophosphatidylserine (LPS) 13:0, LPS 17:1, phosphatidylserine (PS) 14:0/14:0, PS 15:0/18:1-D_7, PS 17:0/17:0, lysophosphatidylglycerol (LPG), 13:0, LPG 14:0, LPG 17:1, LPG 18:0, phosphatidylglycerol (PG) 14:0/14:0, PG 15:0/18:1-D_7, PG 16:0/16:0, PG 17:0/17:0, lysophosphatidylinositol (LPI) 13:0, LPI 17:1, phosphatidylinositol (PI) 15:0/18:1-D_7, PI 16:0/18:2, PI 16:0-D_{31}/18:1, cardiolipin (CL) $(14:0)_4$, CL $(18:2)_4$-D_5, sphingomyelin (SM) d18:1/17:0, SM d18:1/18:1-D_9, ceramide (Cer) d18:1/20:0, Cer d18:1-D_7/24:1, Cer d18:1-D_7/24:0, hexosylceramide (HexCer) d18:1-D_7/15:0, HexCer d18:1/17:0, dihexosylceramide (Hex2Cer) d18:1-D_7/15:0, Hex2Cer d18:1/17:0, diacylglycerol (DG) 15:0_18:1-D_7, DG 16:0_18:1. DG 1,3-18:0-D_5, triacylglycerol (TG) 15:0/18:1-D_7/15:0, TG 17:0/17:1/17:0-D_5, cholesteryl ester (CE) 17:0, and CE 18:1-D_7. In addition, an external standard lipid mixture for establishing calibration curves was prepared using non-endogenous lipids with odd-numbered or deuterium-labelled acyl chains, and an internal standard lipid mixture was developed up by adding eight additional lipid standards (LPG 13:0, LPI 13:0, LPS 13:0, LPA 17:1, CL $(18:2)_4$-D_5, Cer d18:1-D_7/24:0, HexCer d18:1-D_7/15:0, and Hex2Cer d18:1-D_7/15:0) to SPLASH LIPIDOMIX from Avanti Polar Lipids, Inc. For method validation and lipid quantification, all the external and internal lipid standards listed in Table S1 were added to saliva samples prior to lipid extraction. HPLC mobile phase solvents (H_2O, CH_3CN, CH_3OH, and isopropyl alcohol (IPA)) and methyl-*tert*-butyl ether (MTBE) were purchased from Avantor Performance Materials (Center Valley, PA, USA), and ionisation modifiers (NH_4HCO_2 and NH_4OH) and $CHCl_3$ were purchased from Sigma-Aldrich (St. Louis, MO, USA). Capillary columns were prepared using fused silica capillary tubes with an outer diameter (o.d.) of 360 μm and an inner diameter (i.d.) of 100 μm from Polymicro Technology, LLC (Phoenix, AZ, USA). The connection between the UHPLC pump and the analytical column was made using NanoViper capillaries (i.d. 20 μm; from Thermo Scientific (San Jose, CA, USA). The analytical column was packed with two types of packing materials: Watchers ODS-P C-18 particles (3 μm and 100 Å) from Isu Industry Corp. (Seoul, Korea) to form a self-assembled frit at the needle tip of the pulled-tip capillary column and ethylene bridged hybrid (BEH) shield C18 particles (1.7 μm and 130 Å) from Waters (Milford, MA, USA) to pack the remainder of the column. The BEH Shield C18 particles were unpacked using an ACQUITY UPLC BEH Shield C18 column (2.1 mm × 100 mm) from Waters.

2.2. Human saliva samples

Human saliva samples were obtained from 20 healthy volunteers (12 males and 8 females) with a mean age of 30.7 ± 4.2. The healthy volunteers were selected from a population that did not have any major illness or have not taken any drugs in the recent past. For at least 8 h before saliva collection, all volunteers fasted and refrained from dental care, such as brushing teeth or using dental floss, and saliva samples were collected in the period of 9–11 a.m. after volunteers rinsed their mouths with water to remove any other residue. Each saliva sample was collected using a 15 mL Falcon® polypropylene tube from Corning (Glendale, AZ, USA) in our laboratory. At least 1.0 mL of saliva was collected by spitting out from each person. The study was approved by the Institutional Review Board of Severance Hospital (IRB No. 7001988-202105-HR-1216-03) and conducted in accordance with the current version of the Declaration of Helsinki. Collected saliva samples were pooled (1.0 mL from each volunteer) and stored at −80 °C until subjected to lipid extraction.

2.3. Lipid extraction

Prior to lipid extraction, frozen saliva was thawed at room temperature and vortexed for 20 min. Different volumes (1.0, 0.5, 0.2, and 0.1 mL) of the pooled saliva were spiked with external and internal standards and then used for lipid extraction according to a previously reported protocol [24]. For extraction, the spiked saliva samples were lyophilized using a Bondiro MCFD 8508 freeze dryer vacuum centrifuge (IlShinBioBase, Yangju, Korea), dissolved in CH_3OH (300 μL), and cooled in an ice bath for 10 min. Then, MTBE (1000 μL) was added to the mixtures, followed by vortexing for 1 h and the addition of MS-grade H_2O (250 μL), vortexing for another 10 min, and finally centrifuging at 1000×*g* for 10 min. The organic solvent layer that contained lipids was transferred to a new vial. To retrieve additional lipids from the remaining aqueous layer, each solution was mixed with MTBE (300 μL), tip-sonicated for 2 min, and centrifuged at 1000×*g* for 10 min before the resulting organic solvent layer was removed and combined with the previously collected solvent layer. Finally, the combined organic solutions were dried under N_2 gas using an Evatros mini evaporator (Goojung Engineering, Seoul, Korea), and the dried lipids obtained from 1.0, 0.5, 0.2, and 0.1 mL of pooled saliva sample were dissolved in 230, 115, 58, and 29 μL of MeOH:$CHCl_3$:H_2O (18:1:1, v/v/v), respectively. The final lipid suspensions were stored at −80 °C until subjected to further analysis.

Table 1
MS parameter values used for salivary lipid analysis by nUHPLC-ESI-MS/MS.

	MS polarity	
	positive ion mode	negative ion mode
for full MS scan		
Resolution	70,000	70,000
AGC target	1e6	1e6
maximum IT (ms)	200	200
scan range (*m/z*)	400–1100	400–1700
for data dependent MS/MS		
Resolution	17,500	17,500
AGC target	1e5	1e5
maximum IT (ms)	50	50
loop count	10	10
MSX count	1	1
isolation window (*m/z*)	2	2
NCE	22.5	27.5
minimum AGC target	1e4	1e4
dynamic exclusion (s)	1.5	1.5

2.4. Lipidome analysis

Lipid analysis was accomplished in two steps: non-targeted lipid identification and targeted quantification using a nUHPLC-ESI-MS/MS system composed of an Ultimate 3000 RSLCnano System and Q Exactive mass spectrometer from Thermo Scientific (San Jose, CA, USA). To minimise dwell time, the nanoViper capillary tube between the nUHPLC pump and the injection valve of the autosampler was customised to 55 cm long, and another capillary tube between the injection valve and the analytical column was customised to 85 cm long. The pooled-tip analytical column was connected to the nanoViper capillary tube from the injector using a MicroTee from IDEX Health & Science LLC (Oak Harber, WA, USA), in which the remaining port was connected to a Pt wire for ESI voltage. The total dead volume of the nUHPLC system used in the present study was approximately 1623 nL, including the dead volume of the MicroTee (152 nL) and the volume of the sample loop (1 μL) [25].

The analytical column used in the present study was prepared in our laboratory using a fused silica capillary (o.d. 360 μm and i.d. 100 μm). One end of the capillary was pulled into a sharp needle using a torch flame, and a needle-like sharp tip was used as a self-emitter for ESI. The analytical capillary column (80 mm long) was prepared in two steps with N_2 gas at 1000 psi; the column tip was packed with Watchers ODS-P C18 particles (3 μm) for 5 mm to prepare a self-assembled frit, and the remaining column space (~75 mm) was packed with BEH Shield C18 particles (1.7 μm). H_2O:CH_3CN (9:1, v/v) and IPA:CH_3OH:CH_3CN:H_2O (7:1.5:1:0.5, v/v/v/v) were used as mobile phases A and B, respectively, and a mixture of ionisation modifiers (0.5 mM NH_4HCO_2 and 5 mM NH_4OH), which are efficient in both positive and negative ion modes of MS analysis, were added to both mobile phases. An injection volume of 0.3 μL was used for all experiments, and the nUHPLC flow rate was set to 800 nL/min. Analysis included a 30-min gradient elution, beginning with 1% mobile phase B, which was increased to 75% over 5 min, 80% over 5 min, 99% over 5 min, was maintained at 99% for 10 min, reduced to 1%, and then maintained at 1% for 5 min. The ESI voltages applied were 3 kV and 1.5 kV for the positive and negative ion scan modes, respectively.

For global lipid identification, a full MS scan mode with data-dependent MS/MS acquisition was utilised in both positive and negative ion modes. Lipid identification was performed using LipidMatch [26] and the acyl chain positions (sn-1 and sn-2) were manually confirmed using the MS/MS spectra patterns of each lipid class. During manual confirmation of lipid molecular structures, the exact mass of a precursor ion with a tolerance of 5 ppm and retention time were considered.

For lipid quantification, target lipids were selected from the identified list of lipids based on the total numbers of acyl chain carbon and double bond, and targeted quantification was made with a full MS scan of the exact mass of each precursor ion (<5 ppm in tolerance) by considering retention time. Targeted quantification was achieved by scanning both the positive and negative ions alternatively using polarity switching mode in a single nUHPLC run. LPC, PC, EtherLPC, EtherPC, LPE, PE, EtherLPE, EtherPE, SM, Cer, HexCer, Hex2Cer, DG, TG, and CE were detected in the positive ion mode cycle of the polarity switching mode, and LPA, PA, LPS, PS, LPG, PG, LPI, PI, and DLCL were detected in the negative ion cycle. Eight replicate nUHPLC-ESI-MS/MS runs were performed for each sample. Details of the MS parameters used in qualitative and quantitative analyses are listed in Table 1. Individual lipid concentration was calculated using calibration curves established for each lipid class. Molecular identification and quantification were performed using Xcalibur, a software from Thermo Scientific. Calibration curves were established with the normalised peak area

which was the ratio of the peak area of a calibration standard to that of its internal standard (specific to each lipid class) spiked to each saliva sample.

2.5. Method validation

Before lipid extraction, each saliva sample was spiked with a mixture of 20 internal standards with fixed concentrations (0.06–5.77 pmol/μL). For calibration, calibration standard solutions were prepared with a pooled saliva sample by varying the concentration of a mixture of 22 calibration standards at seven different concentrations (0.07, 0.17, 0.33, 1.00, 1.65, 3.33, and 6.67 pmol/μL in Table S1) added with a fixed concentration of the above IS mixture. After lipid extraction, the calibration standards were analysed using five nUHPLC-ESI-MS/MS replicate runs. Based on relative peak area (vs. internal standard), calibration curves were established for each lipid class for each different volume of the pooled saliva sample (i.e., 1.0, 0.5, 0.2, and 0.1 mL). From the calibration parameters including slope and intercept listed in Table S2, LOD and LOQ values were calculated with signal-to-noise ratios (S/N) of 3 and 10, respectively, along with linear range in Table S3a and signals were based on normalised peak area (vs. internal standard).

3. Results and discussion

3.1. Identification of salivary lipids by nUHPLC-ESI-MS/MS

The performance of lipid separation by nUHPLC-ESI-MS/MS is shown with base peak chromatograms of a mixture of lipid standards in Fig. S1, obtained at positive and negative ion modes. With the present nUPHPLC column, a run-to-run repeatability was measured as less than 1% (n = 8) in retention time along with 0.18 min of average peak width. Under the same run conditions utilised in Fig. S1, salivary lipids extracted from four different saliva volumes (1.0, 0.5, 0.2, and 0.1 mL) were analysed using nUHPLC-ESI-MS/MS, and initial saliva volume was found to affect both peak intensities and complexities (Fig. S2). Based on MS/MS analysis of eluted lipids from the 1.0 mL pooled saliva sample 'saliva-1.0', molecular structures of a total of 780 lipids were characterised from their fragment ion spectra. Acyl chain locations (sn-1 and sn-2) were assigned for phospholipids, but only the types of three acyl chains were given for TG without exact locations. The numbers of lipids from each lipid class identified in the saliva-1.0 sample are listed in Table 2, along with the corresponding types of precursor ions detected. A significantly large number of PS species (53 PS and 15 LPS) were detected in saliva since PS is rarely detected in blood plasma (only one PS was reported from the standard reference material 1950 human plasma from National Institute of Standard Technology [27]). This supports the hypothesis that saliva contains both serum-derived and saliva-specific lipids. The identified lipids included constitutional isomers of some lipid classes (e.g., TG and DG) of which different types of acyl chains could be distinguished by MS/MS spectra, but the isomeric species were not individually quantified. The change in the number of quantifiable lipids with the decrease of initial saliva volume is discussed later in this paper.

Table 2
Distribution of lipids in human saliva.

Lipid class	No. identified	Precursor ions
Glycerophospholipids		
LPCs	13	$[M+H]^+/[M+HCO_2]^-$
PCs	42	$[M+H]^+/[M+HCO_2]^-$
LPEs	12	$[M+H]^+/[M-H]^-$
PEs	43	$[M+H]^+/[M-H]^-$
EtherLPCs	19	$[M+H]^+/[M+HCO_2]^-$
EtherPCs	51	$[M+H]^+/[M+HCO_2]^-$
EtherLPEs	4	$[M+H]^+/[M-H]^-$
EtherPEs	24	$[M+H]^+/[M-H]^-$
LPAs	12	$[M-H]^-$
PAs	21	$[M-H]^-$
LPSs	15	$[M-H]^-$
PSs	53	$[M-H]^-$
LPGs	11	$[M-H]^-$
PGs	57	$[M-H]^-$
LPIs	7	$[M-H]^-$
PIs	38	$[M-H]^-$
DLCL	1	$[M-H]^-$
Sphingolipids		
SMs	9	$[M+H]^+/[M+HCO_2]^-$
Cers	31	$[M+H]^+/[M+HCO_2]^-$
HexCers	10	$[M+H]^+/[M+HCO_2]^-$
Hex2Cers	4	$[M+H]^+/[M+HCO_2]^-$
Glycerolipids		
DGs	35	$[M+NH_4]^+$
TGs	264	$[M+NH_4]^+$
Sterol lipids		
CEs	4	$[M+NH_4]^+$
Total	780	

3.2. Extraction recovery and matrix effect

Extraction recovery, R_E (%), was calculated as follows: R_E (%) = $A_{sb}/A_{sa} \times 100$, where A_{sb} and A_{sa} represent the normalised peak areas (vs. IS) of a lipid standard (0.17 pmol/μL for each lipid class) spiked into the pulled saliva sample before and after extraction, respectively. Matrix effect, *ME (%)*, was calculated as follows: $ME\,(\%) = (A_{sa}/A_n - 1) \times 100$, where A_n is the peak area of the same lipid standard in a neat solution (no extraction) [24]. The calculated R_E and *ME* values are listed in Table 3, along with the relative standard deviation values. Mean R_E was less than 110% for the saliva-1.0 (108.8 ± 14.3%), saliva-0.5 (102.3 ± 14.0%) (0.5 represents volume of saliva hereafter), and saliva-0.2 (96.9 ± 13.9%) samples, but the mean R_E for the saliva-0.1 samples (116.4 ± 14.0%) was relatively poor. A negative *ME* value indicates the suppression of ionisation, and a positive value represents the signal enhancement of an analyte. The *ME* values indicated that a severe ionisation suppression occurred in most lipid classes when 1.0 mL of saliva was used for extraction, which is evidence of the matrix effect. In addition, the matrix effect appeared to be correlated with saliva sample volume. However, this needs to be examined together with the efficiency of lipid quantitation.

3.3. Efficiency of lipid quantitation

First, the effect of initial saliva volume on the LOD of each saliva was evaluated using the calibration curve parameters listed in Table S2. Based on the Mandel's fitting test, the linearity of each calibration curve was confirmed. The LOD of each lipid class was calculated as follows: LOD = 3 × (SD of y-intercept/slope of calibration curve). LOD values ranged from 0.02 (PG 17:0/17:0 for the saliva-0.1 sample) to 0.33 pmol/μL (PS 17:0/17:0 for the saliva-1.0 sample) and LOQ values ranged from 0.08 (PG 17:0/17:0 for the saliva-0.1 sample) to 1.10 pmol/μL (PS 17:0/17:0 for the saliva-1.0 sample) (Table S3a). The LOD and LOQ values for most of the lipid classes were about three times greater in the saliva-1.0 sample than in the lower volume samples, which shared similar values. This indicated that the matrix effect increased significantly with an initial sample volume 1.0 mL but was less severe with initial sample volumes up to 0.5 mL. Accuracy (relative error, %) and precision (CV, %) in the calculation of concentration of each lipid standard are listed in Table S3b, showing 5.1–6.3% in average and 5.4–8.6% in average, respectively. Column-to-column reproducibility was

Table 3
Evaluation of optimal initial sample volume for salivary lipid extraction based on extraction recovery (R_E, %), matrix effect (*ME*, %), and relative standard deviation (RSD, %) of each lipid standard (0.17 pmol/μL) spiked into saliva (n = 5).

	R_E (%)				*ME* (%)				RSD (%)			
Lipid standard	1.0 mL	0.5 mL	0.2 mL	0.1 mL	1.0 mL	0.5 mL	0.2 mL	0.1 mL	1.0 mL	0.5 mL	0.2 mL	0.1 mL
LPC 17:1	96.0	90.0	93.9	113.0	−13.8	−6.7	3.7	1.1	2.4	5.9	6.5	3.4
PC 17:0/17:0	133.8	92.6	121.0	101.2	−25.2	9.4	1.3	10.4	3.6	1.2	11.8	5.4
LPE 17:1	103.5	98.9	95.5	124.5	−15.2	1.2	1.2	3.4	4.9	3.9	4.5	4.2
PE 17:0/17:0	130.6	105.8	118.6	127.4	−9.5	−4.4	2.1	8.6	3.9	3.3	2.6	7.0
LPG 17:1	117.5	143.7	119.5	137.9	−11.6	−3.1	−1.0	6.1	5.5	12.9	11.9	4.3
PG 17:0/17:0	109.9	108.3	96.1	122.9	−9.5	−3.6	−0.2	0.7	10.5	6.3	6.1	1.9
LPI 17:1	109.1	118.1	112.2	108.7	−3.9	0.5	3.3	3.0	8.2	7.1	4.2	12.5
PI 16:0 (d31)/18:1	106.0	80.6	84.9	122.0	−2.4	2.4	3.4	0.2	7.7	6.2	8.0	9.2
LPS 17:1	123.1	119.7	114.0	120.5	−14.1	0.6	0.6	9.8	7.0	11.5	11.5	3.1
PS 17:0/17:0	77.9	99.4	84.2	116.2	−16.1	−8.6	0.5	7.7	5.1	2.2	11.6	4.3
LPA 17:0	92.3	99.6	114.0	126.2	−1.9	1.3	−2.9	7.1	12.9	11.0	8.8	14.1
PA 17:0/17:0	90.2	99.7	75.5	95.2	−9.7	−4.7	2.4	9.6	2.1	9.8	4.2	13.7
EtherPE P-18:0/18:1(d9)	107.8	107.8	78.1	133.9	−34.4	−9.9	−0.3	7.0	8.2	4.5	7.8	2.0
EtherPC P-18:0/18:1(d9)	115.1	90.4	86.5	121.0	−7.7	2.9	−4.6	−3.0	13.0	5.6	9.0	8.9
CL $(18:2)_4$ (d5)	98.9	82.3	93.8	77.9	−29.7	−10.5	−1.1	3.2	7.5	10.3	7.8	7.9
Cer d18:1 (d7)/24:1	108.5	98.4	89.9	124.9	−32.7	−4.2	0.4	4.3	3.3	2.8	7.0	6.3
SM d18:1/17:0	99.7	100.8	90.0	104.0	−13.7	−8.1	0.3	8.2	6.4	6.5	11.2	7.0
HexCer d18:1/17:0	111.5	109.5	104.2	113.5	−5.2	0.1	9.2	5.9	2.9	10.8	12.5	4.4
Hex2Cer d18:1/17:0	122.0	84.3	97.5	107.4	−17.3	4.9	8.9	10.9	14.7	11.0	10.6	4.9
DG 1,3−18:0 (d5)	92.4	109.5	86.5	115.6	−18.4	−3.2	2.2	9.1	12.5	14.1	7.9	4.7
TG 17:0/17:1/17:0 (d5)	123.7	105.1	90.4	110.5	−15.7	0.2	2.5	5.8	3.6	3.9	5.5	4.1
CE 17:0	125.0	106.9	85.5	135.5	−26.2	1.1	1.4	4.1	17.1	12.7	2.5	4.0

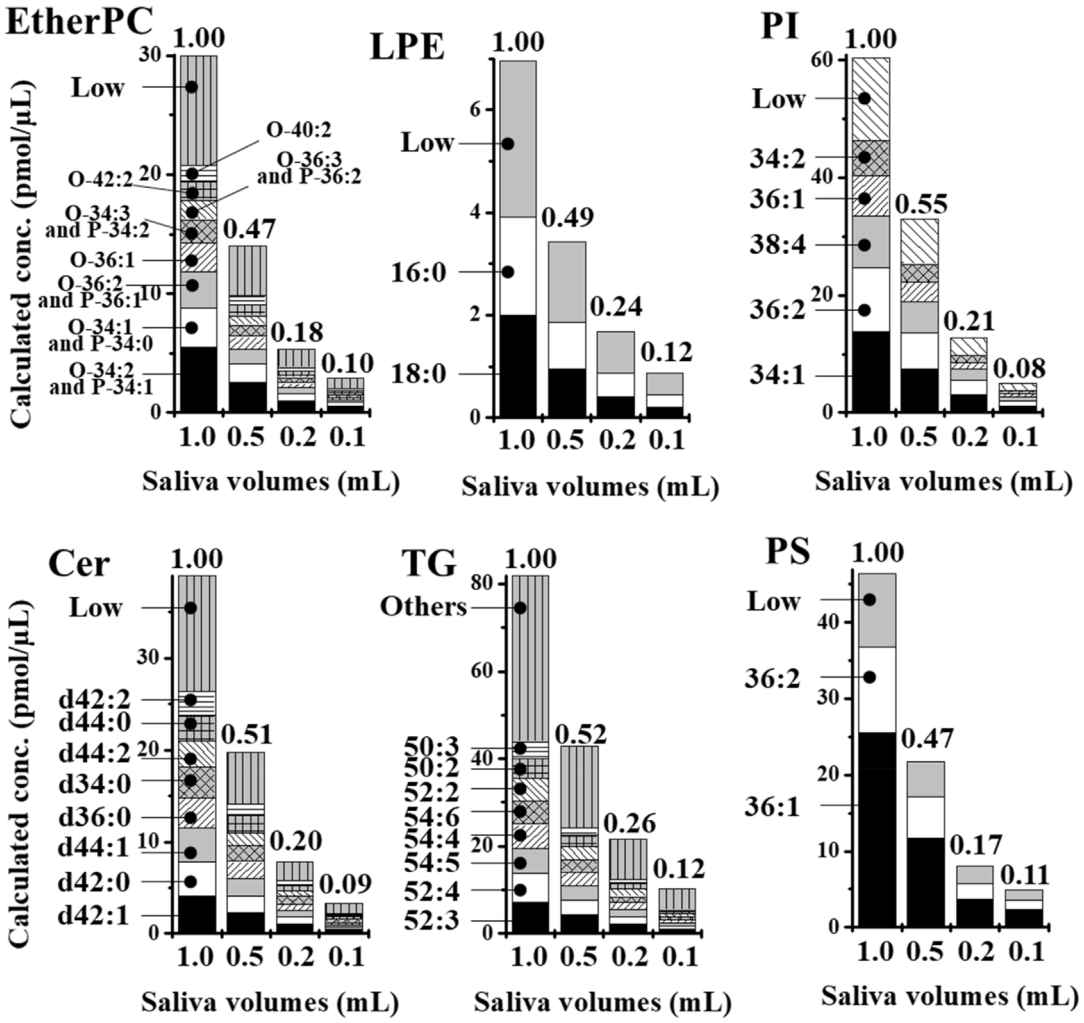

Fig. 1. Effect of initial sample volume on the relative concentrations of salivary lipid species. Number above each chart represents the total concentration of each class relative to that of the saliva-1.0 sample.

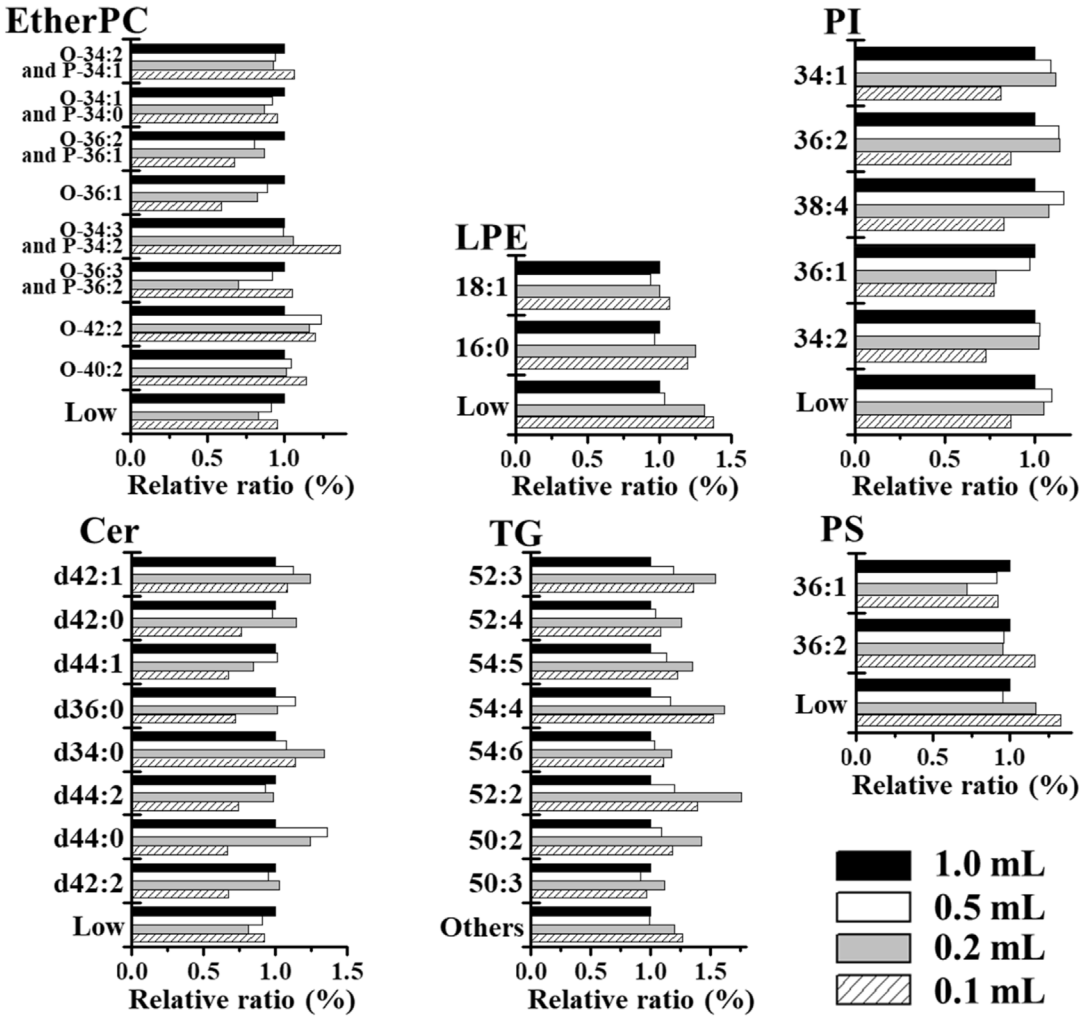

Fig. 2. Effect of initial sample volume on the distribution of most abundant salivary lipids.

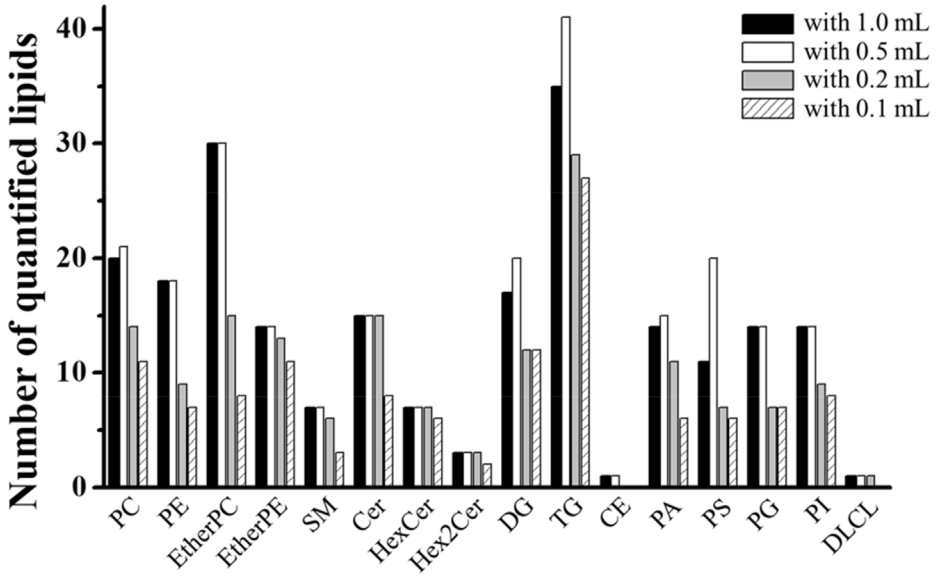

Fig. 3. Effect of initial sample volume on the number of quantifiable salivary lipids.

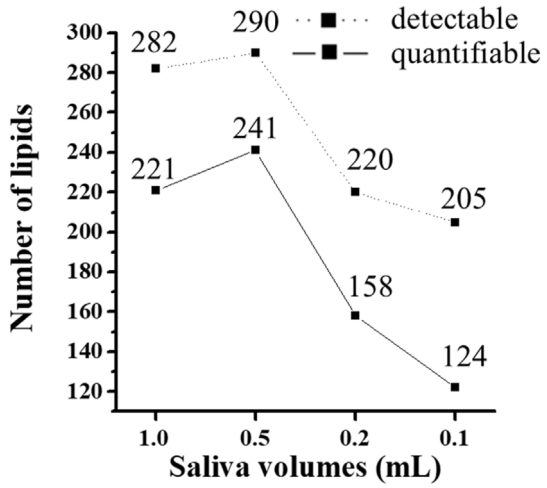

Fig. 4. Effect of initial sample volume on the number of detectable and quantifiable salivary lipids.

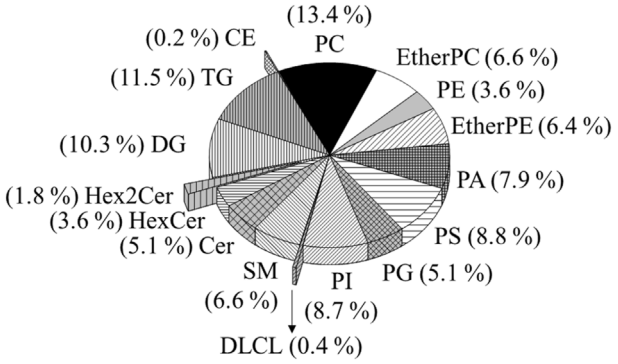

Fig. 5. Distribution of lipid classes quantified in 0.5 mL saliva using nanoflow ultrahigh performance liquid chromatography-tandem mass spectrometry (nUHPLC-ESI-MS/MS).

calculated to be 2.3% (average for 20 standards, n = 3) expressed with relative standard deviation of retention times (Table S3b).

The concentration of an individual lipid calculated using calibration curves is listed in Table S4, along with the relative abundance value in each class. For instance, the abundance value represents the relative abundance of a species in each lipid class and a species with underlined abundance is a high abundance lipid in its class. High abundance was defined when a relative abundance of a species was larger than 100% divided by the total number of quantified lipids in its lipid class. For instance, the relative abundance of LPC 18:1 was 33.86% which was a high abundance species since it was larger than 7.69% (= 100%/13 LPCs). Since lipid quantitation was performed with identified targets based on full MS scan within 5 ppm in tolerance and retention time, quantified results were represented by lipid species with the total chain length and the number of double bonds (i.e. PC 36:1) in Table S4. The isomeric structures of all the identified lipid species are listed in Table S5. The effect of initial sample volume on the concentrations of individual lipid species is illustrated in Fig. 1. In Fig. 1, the lipid species marked with acyl chain information belong to a high-abundance species in each class, and the bar graph marked with 'Low' represents the summed amount of all low-abundance species in each class. The concentration profiles of the 15 remaining lipid classes are plotted in Fig. S3. Even though the effect of initial sample volume on the levels of individual lipid species was not immediately clear (Fig. 1), the changes in the total level of each lipid class were more easily recognised. It is expected that total level of each lipid class decreases as much as the decrease of saliva volume used for extraction. The total levels of LPE, PI, and TG were increased by >10% when initial sample volume was reduced, which suggested that the matrix effect was greater when using 1.0 mL saliva than when using lower volumes. Several other lipid classes exhibited similar patterns (Fig. S3). Changes at the individual level are represented in Fig. 2 by plotting the relative amount of each species (in comparison to the concentration of the same species from the saliva-1.0) multiplied by the volume factor (1, 2, 5, and 10 for the saliva-1.0, 0.5, −0.2, and −0.1). Plots of the lipid classes that are not shown in Fig. 2 are shown in Fig. S4. The relative abundance values of most lipid species from the saliva-0.5 and saliva-1.0 samples were similar, whereas those from the saliva-0.2 and saliva-0.1 samples were significantly lower, which could be attributed to the poor detection of low-abundance species.

The effect of saliva volume on the quantifiable number of lipids was examined by counting lipids with concentrations above the LOQ (S/N > 10). The number of quantifiable PC, DG, TG, PA, and PS lipids increased initially but decreased for most lipid classes with further reduction in initial saliva volume (Fig. 3). A total of 241 lipids were quantifiable using the initial sample volume of 0.5 mL (Fig. 4). Number of detectable lipids (S/N > 3) exhibited a similar pattern.

Finally, the relative composition of the lipid class is plotted in Fig. 5 based on the quantified lipids from the saliva-0.5 sample. PC was the most abundant class of lipids recovered from the pooled saliva sample (13.4%), followed by TG (11.5%), DG (10.3%), and PS (8.8%). The distribution of lipid species among typical categories was as follows: 60.9% for glycerophospholipids, 21.8% for glycerolipids, 17.1% for sphingolipids, and 0.2% for sterol lipids. As discussed briefly above, PSs accounted for 8.8% of the total lipids quantified. A previous study [28] has reported that PSs accounts for 11.4% of the total phospholipids in labial salivary gland secretions. Excluding glycerolipids, the lipid composition data observed here were almost identical to those reported in the literature (PC: 16.3%, PA 8.1%, and PG 5.2%) [28]. Since the nUHPLC-ESI-MS/MS run conditions used in the present study were well-tuned to the detection of glycerophospholipids, sphingolipids, and glycerolipids, the actual composition of sterol lipids might not be accurately evaluated.

4. Conclusions

Despite the facts that saliva contains bio-informative molecules, such as proteins and metabolites (e.g., lipids), that are similar to those found in serum and that its collection is simple and non-invasive, the dilute nature of saliva has discouraged its use for the development of biomarkers candidates for the diagnosis and prognosis of diseases. In the present study, the effect of initial saliva sample volume on the efficiency of lipid extraction and lipidomic analysis was evaluated by assessing extraction efficiency, matrix effect, LOD, and the numbers of detectable and quantifiable lipids using nUHPLC-ESI-MS/MS. Extraction recovery was relatively unaffected by initial sample volume, whereas the matrix effect and initial volume were positively related. By considering extraction recovery, matrix effect, and maximum number of quantifiable lipids, an optimal initial sample volume of 0.5 mL was selected. Because this result was specific to the use of nUHPLC-ESI-MS/MS, lipidomic analyses with larger columns might require larger extraction volumes. While this study utilised the pooled saliva sample from several individuals in order to prepare a stock to carry out optimizations, it demonstrates that lipid profiles can be analysed with only a small volume (0.5 mL) of saliva from individuals.

Moreover, this study demonstrated a method for the comprehensive lipid analysis of saliva and provided a useful guideline for large scale (in terms of sample number) lipidomic analyses, thereby promoting the use of salivary lipids in biomarker discovery and disease screening.

CRediT authorship contribution statement

Gwang Bin Lee: Formal analysis, Methodology, Writing – original draft, Data curation. **Ayse Caner:** Conceptualization. **Myeong Hee Moon:** Supervision, Writing – review & editing.

Declaration of competing interest

The authors declare that they have no known competing financial interests or personal relationships that could have appeared to influence the work reported in this paper.

Acknowledgements

Role of the funding source: This work was supported by a bilateral research program (NRF-2020K2A9A1A06097918) between Turkey and Korea supported by the National Research Foundation (NRF) of Korea and in part by NRF-2021R1A2C2003171.

Appendix A. Supplementary data

Supplementary data to this article can be found online at https://doi.org/10.1016/j.aca.2021.339318.

References

[1] S. Agatonovic-Kustrin, D.W. Morton, V. Smirnov, A. Petukhov, V. Gegechkori, V. Kuzina, N. Gorpinchenko, G. Ramenskaya, Analytical strategies in lipidomics for discovery of functional biomarkers from human saliva, Dis. Markers 2019 (2019), 6741518.
[2] S.P. Humphrey, R.T. Williamson, A review of saliva: normal composition, flow, and function, J. Prosthet. Dent 85 (2) (2001) 162–169.
[3] Y. Tomita, N. Miyake, S. Yamanaka, Lipids in human parotid saliva with regard to caries experience, J. Oleo Sci. 57 (2) (2008) 115–121.
[4] L.R. Bigler, C.F. Streckfus, W.P. Dubinsky, Salivary biomarkers for the detection of malignant tumors that are remote from the oral cavity, Clin. Lab. Med. 29 (1) (2009) 71–85.
[5] L. Samaranayake, Saliva as a diagnostic fluid, Int. Dent. J. 57 (5) (2007) 295–299.
[6] A.H. Zhang, H. Sun, X.J. Wang, Saliva metabolomics opens door to biomarker discovery, disease diagnosis, and treatment, Appl. Biochem. Biotechnol. 168 (6) (2012) 1718–1727.
[7] M. Esteban, A. Castano, Non-invasive matrices in human biomonitoring: a review, Environ. Int. 35 (2) (2009) 438–449.
[8] E. Neyraud, M. Tremblay-Franco, S. Gregoire, O. Berdeaux, C. Canlet, Relationships between the metabolome and the fatty acid composition of human saliva; effects of stimulation, Metabolomics 9 (1) (2013) 213–222.
[9] A. Aguirre, L.A. Testa-Weintraub, J.A. Banderas, G.G. Haraszthy, M.S. Reddy, M.J. Levine, Sialochemistry: a diagnostic tool? Crit. Rev. Oral Biol. Med. 4 (3–4) (1993) 343–350.
[10] L.A. Aqrawi, H.K. Galtung, B. Vestad, R. Ovstebo, B. Thiede, S. Rusthen, A. Young, E.M. Guerreiro, T.P. Utheim, X. Chen, O.A. Utheim, O. Palm, J.L. Jensen, Identification of potential saliva and tear biomarkers in primary Sjogren's syndrome, utilising the extraction of extracellular vesicles and proteomics analysis, Arthritis Res. Ther. 19 (1) (2017) 1–15.
[11] M. Tiwari, Science behind human saliva, J. Nat. Sci. Biol. Med. 2 (1) (2011) 53–58.
[12] P. Jacob 3rd, L. Yu, M. Duan, L. Ramos, O. Yturralde, N.L. Benowitz, Determination of the nicotine metabolites cotinine and trans-3'-hydroxycotinine in biologic fluids of smokers and non-smokers using liquid chromatography-tandem mass spectrometry: biomarkers for tobacco smoke exposure and for phenotyping cytochrome P450 2A6 activity, J Chromatogr B Analyt Technol Biomed Life Sci 879 (3–4) (2011) 267–276.
[13] M.R. Djordje Bozovic, Nedeljka ivkovic, salivary cortisol levels as a biological marker of stress reaction, Med. Arch. 67 (5) (2013) 371–374.
[14] M.-P. Martinez-Moral, K. Kannan, How stable is oxidative stress level? An observational study of intra- and inter-individual variability in urinary oxidative stress biomarkers of DNA, proteins, and lipids in healthy individuals, Environ. Int. 123 (2019) 382–389.
[15] C. Hirtz, J. Vialaret, N. Nowak, A. Gabelle, D.D. de Periere, S. Lehmann, Absolute quantification of 35 plasma biomarkers in human saliva using targeted MS, Bioanalysis 8 (1) (2016) 43–53.
[16] S. Singh, V. Ramesh, N. Oza, P. Balamurali, K. Prashad, P. Balakrishnan, Evaluation of serum and salivary lipid profile: a correlative study, J. Oral Maxillofac. Pathol. 18 (1) (2014) 4–8.
[17] S.L. Veena Kalburgi, Shivaraj Warad, Saliva as a surrogate to explore the association between lipid profiles and chronic periodontitis: a case-control study, Dent. Res. J. 11 (6) (2014) 619–623.
[18] M.R. Wenk, Lipidomics: new tools and applications, Cell 143 (6) (2010) 888–895.
[19] M. Holcapek, G. Liebisch, K. Elcroos, Lipidomic analysis, Anal. Chem. 90 (7) (2018) 4249–4257.
[20] J.C. Lee, I.Y. Kim, Y. Son, S.K. Byeon, D.H. Yoon, J.S. Son, H.S. Song, W. Song, J.K. Seong, M.H. Moon, Evaluation of treadmill exercise effect on muscular lipid profiles of diabetic fatty rats by nanoflow liquid chromatography-tandem mass spectrometry, Sci Rep-Uk 6 (1) (2016) 1–14.
[21] S.H. Kim, J.S. Yang, J.C. Lee, J.-Y. Lee, J.-Y. Lee, E. Kim, M.H. Moon, Lipidomic alterations in lipoproteins of patients with mild cognitive impairment and Alzheimer's disease by asymmetrical flow field-flow fractionation and nanoflow ultrahigh performance liquid chromatography-tandem mass spectrometry, J. Chromatogr. A 1568 (2018) 91–100.
[22] J.H. Lee, J.S. Yang, S.H. Lee, M.H. Moon, Analysis of lipoprotein-specific lipids in patients with acute coronary syndrome by asymmetrical flow field-flow fractionation and nanoflow liquid chromatography-tandem mass spectrometry, J. Chromatogr. B 1099 (2018) 56–63.
[23] G.B. Lee, J.C. Lee, M.H. Moon, Plasma lipid profile comparison of five different cancers by nanoflow ultrahigh performance liquid chromatography-tandem mass spectrometry, Anal. Chim. Acta 1063 (2019) 117–126.
[24] D.Y. Bang, S.K. Byeon, M.H. Moon, Rapid and simple extraction of lipids from blood plasma and urine for liquid chromatography-tandem mass spectrometry, J. Chromatogr. A 1331 (2014) 19–26.
[25] J.C. Lee, Y.B. Kim, M.H. Moon, Enhancement of acidic lipid analysis by nanoflow ultrahigh performance liquid chromatography–mass spectrometry, Anal. Chim. Acta 1166 (338573) (2021) 1–10.
[26] J.P. Koelmel, N.M. Kroeger, C.Z. Ulmer, J.A. Bowden, R.E. Patterson, J.A. Cochran, C.W.W. Beecher, T.J. Garrett, R.A. Yost, LipidMatch: an automated workflow for rule-based lipid identification using untargeted high-resolution tandem mass spectrometry data, BMC Bioinf. 18 (1) (2017) 1–11.
[27] J.A. Bowden, A. Heckert, C.Z. Ulmer, C.M. Jones, J.P. Koelmel, L. Abdullah, L. Ahonen, Y. Alnouti, A.M. Armando, J.M. Asara, T. Bamba, J.R. Barr, J. Bergquist, C.H. Borchers, J. Brandsma, S.B. Breitkopf, T. Cajka, A. Cazenave-Gassiot, A. Checa, M.A. Cinel, R.A. Colas, S. Cremers, E.A. Dennis, J.E. Evans, A. Fauland, O. Fiehn, M.S. Gardner, T.J. Garrett, K.H. Gotlinger, J. Han, Y. Huang, A.H. Neo, T. Hyotylainen, Y. Izumi, H. Jiang, H. Jiang, J. Jiang, M. Kachman, R. Kiyonami, K. Klavins, C. Klose, H.C. Kofeler, J. Kolmert, T. Koal, G. Koster, Z. Kuklenyik, I.J. Kurland, M. Leadley, K. Lin, K.R. Maddipati, D. McDougall, P.J. Meikle, N.A. Mellett, C. Monnin, M.A. Moseley, R. Nandakumar, M. Oresic, R. Patterson, D. Peake, J.S. Pierce, M. Post, A.D. Postle, R. Pugh, Y. Qiu, O. Quehenberger, P. Ramrup, J. Rees, B. Rembiesa, D. Reynaud, M.R. Roth, S. Sales, K. Schuhmann, M.L. Schwartzman, C.N. Serhan, A. Shevchenko, S.E. Somerville, L. St John-Williams, M.A. Surma, H. Takeda, R. Thakare, J.W. Thompson, F. Torta, A. Triebl, M. Trotzmuller, S.J.K. Ubhayasekera, D. Vuckovic, J.M. Weir, R. Welti, M.R. Wenk, C.E. Wheelock, L. Yao, M. Yuan, X.H. Zhao, S. Zhou, Harmonizing lipidomics: NIST interlaboratory comparison exercise for lipidomics using SRM 1950-Metabolites in Frozen Human Plasma, J. Lipid Res. 58 (12) (2017) 2275–2288.
[28] B.L. Slomiany, E. Zdebska, V.L.N. Murty, A. Slomiany, K. Petropoulou, I.D. Mandel, Lipid-composition of human labial salivary-gland secretions, Arch. Oral Biol. 28 (8) (1983) 711–714.